Journal of Organometallic Chemistry 693 (2008) 3387–3395

Contents lists available at ScienceDirect

Journal of Organometallic Chemistry

journal homepage: www.elsevier.com/locate/jorganchem

Experimental and density functional theory (DFT) studies on the DNA-binding trend and spectral properties of two new Ru(II) complexes: $[Ru(L)_2(mip)](ClO_4)_2$ (L = 2,9-dmp and 4,7-dmp)

Lifeng Tan [a,b,*], Sheng Zhang [a], Xiaohua Liu [c], Yuandao Chen [d], Xuewen Liu [d]

[a] College of Chemistry, Xiangtan University, Xiangtan 411105, PR China
[b] Key Lab of Environment-Friendly Chemistry and Application in Ministry of Education, Xiangtan University, Xiangtan 411105, PR China
[c] College of Chemical Engineering, Xiangtan University, Xiangtan 411105, PR China
[d] Department of Chemistry and Chemical Engineering, Hunan University of Arts and Science, Changde 415000, PR China

ARTICLE INFO

Article history:
Received 1 May 2008
Received in revised form 24 July 2008
Accepted 29 July 2008
Available online 5 August 2008

Keywords:
Ruthenium(II) complex
Polypyridyl ligand
DNA-binding
Photocleavage
Density functional theory

ABSTRACT

The new ligand 2′-(3″,4″-methylene-dioxyphenyl)imidazo[4′,5′-*f*] [1,10]phenanthroline (mip) and its Ru(II) complexes $[Ru(2,9\text{-dmp})_2(mip)]^{2+}$ (**1**) (2,9-dmp = 2,9-dimethyl-1,10-phenanthrolline) and $[Ru(4,7\text{-dmp})_2(mip)]^{2+}$ (**2**) (4,7-dmp = 4,7-dimethyl-1,10-phenanthrolline) were synthesized and characterized. The binding properties of the two complexes to calf-thymus DNA (CT-DNA) were investigated by different spectrophotometric methods and viscosity measurements. Both **1** and **2** bind to CT-DNA in an intercalative mode, but with different binding strengths. Complex **2** can emit luminescence in the Tris buffer at ambient temperature, however, complex **1** showed no fluorescence emission, neither alone nor in the presence of CT-DNA. The circular-dichroism signal of the dialysate of the racemic complex against CT-DNA suggests that complexes **1** and **2** interact enantioselectively with CT-DNA. Furthermore, complexes **1** and **2** have been found to be an efficient photosensitiser for cracking DNA plasmid. Theoretical calculations for **1** and **2** were also carried out applying the density functional theory (DFT) method and applied to explain some obtained experimental observations.

1. Introduction

In recent years, tremendous interest has been aroused to explore the potential applications of metal complexes as non-radioactive probes of nucleic acid structure and as possible DNA cleaving agents [1–3]. In particular, Ru(II) complexes with polypyridyl ligands, due to a combination of easily constructed rigid chiral structures spanning all three spatial dimensions and a rich photophysical repertoire, have attracted considerable attention [4–10]. $[Ru(phen)_2dppz]^{2+}$ (dppz = dipyrido-[3,2-*a*:2′,3′-*c*]phenazine) shows no photoluminescence in aq. solution at ambient temperature but luminescence brightly upon binding intercalatively with the dppz ligand between adjacent DNA base pairs, displaying the characteristic of molecular 'light switch' [2,11]. However, there is still no consensus regarding the orientation and/or the location (major or minor groove) of the enantiomers binding with DNA, and the binding mode of the prototype complex $[Ru(phen)_3]^{2+}$ (phen = 1,10-phenanthroline) remains an issue of vigorous debate [12–16]. Therefore, the binding of Ru(II) polypyridyl complexes to DNA has initiated vigorous interest and many structural analogues based on the prototype $[Ru(phen)_3]^{2+}$ have been also synthesized and investigated.

However, it is noted that most of these reported complexes contain only planararomatic ligands, and investigations of such complexes with ligands containing substituent as DNA-binding reagents have been relatively few. In fact, some of these complexes also exhibit interesting properties upon binding to DNA [17–19]. In order to obtain more insights into the DNA-binding and photocleavage properties of Ru(II) complexes, a novel polypyridyl ligand 2′-(3″,4″-methylene-dioxyphenyl) imidazo[4′,5′-*f*][1,10]phenanthroline (mip) and its Ru(II) complexes $[Ru(2,9\text{-dmp})_2(mip)]^{2+}$ (**1**) and $[Ru(4,7\text{-dmp})_2(mip)]^{2+}$ (**2**) (Scheme 1) were synthesized and characterized. The binding properties of the complexes to calf-thymus DNA (CT-DNA) have been studied by spectrophotometric methods and viscosity measurements. The DNA-binding constants K_b of complexes **1** and **2** were measured to be $(2.1 \pm 0.12) \times 10^4\ M^{-1}$ and $(4.1 \pm 0.15) \times 10^4\ M^{-1}$, respectively. The results show that the DNA-binding affinity of complex **1** becomes weaker in intercalation mode than complex **2** does. Theoretical explanation on the difference of DNA-binding affinity of complexes **1** and **2** were also carried out to applying the density functional theory (DFT) method. Furthermore, the abilities of

* Corresponding author. Address: College of Chemistry, Xiangtan University, Xiangtan 411105, PR China. Tel.: +86 732 8293997; fax: +86 732 8292477.
E-mail address: lfwyxh@yahoo.com.cn (L. Tan).

0022-328X/$ - see front matter © 2008 Elsevier B.V. All rights reserved.
doi:10.1016/j.jorganchem.2008.07.033

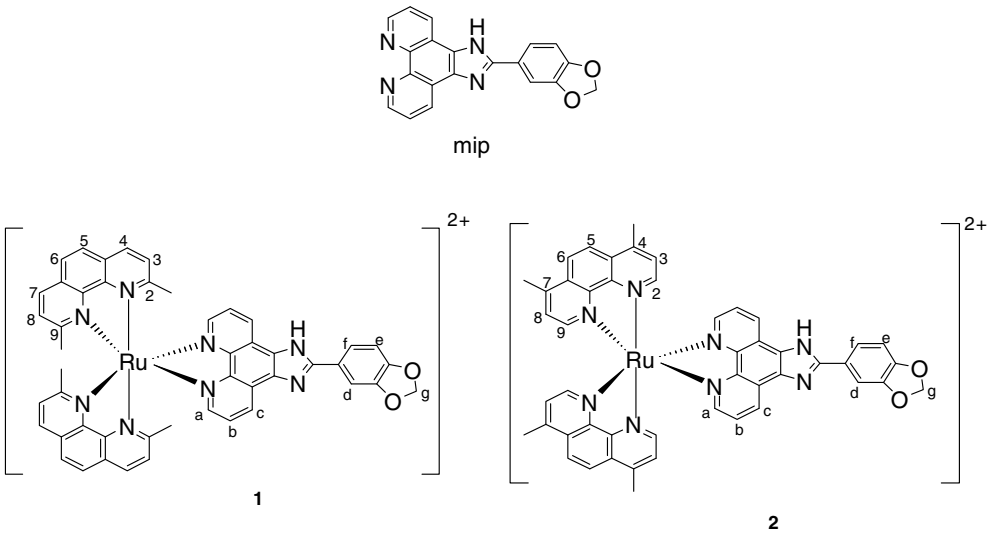

Scheme 1. Structures of the ligand mip and its Ru(II) complexes **1** and **2**.

complexes **1** and **2** to induce the cleavage of pBR-322 DNA were also investigated. We hope that our results will aid in the understanding of DNA recognition and binding by Ru(II) complexes, as well as laying the foundation for the rational design of new photoprobes and photonucleases for DNA.

2. Experimental

2.1. General procedures

All reagents and solvents were commercially available and used without further purification, unless noted otherwise. Doubly distilled H_2O was used to prepare buffers. CT-DNA was obtained from the *Sino-American Biotechnology Company*. *cis*-[Ru(2,9-dmp)$_2$Cl$_2$] · 2H$_2$O [20], *cis*-[Ru(4,7-dmp)$_2$Cl$_2$] · 2H$_2$O [21] and 5,6-dione-1,10-phenan-throline [22] were prepared according to literature procedures. All other materials were commercially available and reagent-grade.

Microanalyses (C, H and N) were carried out on Perkin–Elmer 240Q elemental analyzer. ^{1}H NMR spectra were recorded on Avance-400 spectrometer with d_6-DMSO (dimethyl sulfoxide) as solvent at room temperature and TMS (tetramethylsilane) as the internal standard. UV–Vis (UV–Vis) spectra were recorded on Perkin–Elmer Lambda-25 spectrophotometer, and emission spectra were recorded on Perkin–Elmer LS-55 luminescence spectrometer at room temperature. Fast atom bombardment mass spectra (FAB-MS) were recorded on VG ZAB-HS spectrometer in a 3-nitrobenzyl alcohol matrix. Electrospray mass spectra (ES–MS) were recorded on LQC system (Finngan MAT, USA) using CH_3CN as mobile phase. The spray voltage, tube lens offset, capillary voltage and capillary temperature were set at 4.50 kV, 30.00 V, 23.00 V and 200 °C, respectively, and the quoted *m*/*z* values are for the major peaks in the isotope distribution. Circular-dichroism (CD) spectra were measured on JASCO-J715 spectropolarimeter.

The electrochemical characteristics of the complex were investigated using cyclic voltammetry. All voltammograms were obtained with an Autolab PGSTAT30 electrochemical system. The electrochemical measurements were made in a typical cell using a platinum wire working electrode, and a standard saturated sodium calomel electrode (SSCE). The supporting electrolyte was 0.1 mol/L tetrabutylammonium (Nbu_4) perchlorate. All samples were purged with nitrogen prior to measurement at room temperature. Scan rate of all voltammograms was 200 mV/s.

2.2. DNA-binding and photocleavage experiments

All experiments were carried out in buffer A (5 mm *Tris*·HCl, 50 mm NaCl, pH 7.2) at r.t. A solution of CT-DNA in buffer A gave a ratio of UV absorbances at 260 and 280 nm of *ca.* 1.8–1.9:1, indicating that the DNA was sufficiently free of protein [23]. The concentration of calf-thymus DNA (CT-DNA) per nucleotide was determined spectrophotometrically (ε_{260} = 6600 M^{-1} cm^{-1}) [24]. Stock solutions were stored at 4 °C, and used within 4 d. Titration experiments were performed at a fixed complex concentration (10 μm), to which CT-DNA stock solution was added up to a [DNA]/[Ru] ratio of 1:1. The mixture was allowed to equilibrate for 5 min before spectra were recorded.

The viscosity experiments were carried out with an *Ubbelodhe* viscometer maintained at 25.0 ± 0.1 °C in a thermostated bath. DNA Samples of *ca.* 200-bp average length were prepared by sonication [25]. The flow time was measured with a digital stopwatch, and each sample was tested three times to get an average calculated time. Data are presented as $(\eta/\eta_0)^{1/3}$ versus binding ratio [26], where η is the viscosity of DNA in the presence of the appropriate complex, η_0 being the viscosity of free DNA.

For the gel electrophoresis experiments, supercoiled pBR-322 DNA (0.1 μg) was treated with Ru(Π) complexes in buffer B (50 mM Tris–HCl, 18 mM NaCl, pH 7.2), and the solutions were then irradiated at room temperature with a UV lamp (16 W, 365 nm). The samples were analyzed by electrophoresis for 1 h at 75 V on a 1% agarose gel in Tris-acetate buffer. The gel was stained with ethidium bromide and photographed under UV light.

2.3. Theoretical calculations

The structural schemes of the novel complex [Ru(2,9-dmp)$_2$(mip)]$^{2+}$ **1** and its parent complex [Ru(4,7-dmp)$_2$(mip)]$^{2+}$ **2** for comparison were shown in Scheme 1. Each of them forms from a Ru^{II} ion, one main (intercalative) ligand (mip) and two same ancillary liands (2,9-dmp or 4,7-dmp). Full geometry optimization computations were performed applying the DFT-B3LYP method and Land2DZ basis set [27,28], and assuming the single state for the ground state of the complexes [29]. All computations were performed with the G98 quantum chemistry program-package [30]. In order to vividly depict the detail of the frontier molecular orbital interactions, the stereographs of some related frontier molecular orbitals of the complexes were drawn with the

MOLDEN v3.7 program [31] based on the obtained computational results.

2.4. Preparation of mip

A mixture of 3,4-methylenedioxy-benzaldehyde (0.45 g, 3 mM), 1,10-phenanthroline-5,6-dione (0.21 g, 3 mmol), ammonium acetate (4.62 g, 60 mM) and glacial acetic acid (30 ml) was heated at reflux with stirring for 2 h. The solution was allowed to cool, filtered, diluted with H_2O, and neutralized with conc. aq. NH_3. The orange precipitate was collected and purified by column chromatography on alumina with ethanol–toluene (16:1 v/v) as eluent to give the title compound as amorphous yellow solid.

Yield: 0.52 g (47%). ^{1}H NMR (400 MHz, (D_6)DMSO): δ = 13.56 (br, s, 1H), 9.10 (dd, 2H), 8.91(d, 2H), 7.84 (m, 2H), 7.80 (m, 2H), 7.18 (d, 1H), 6.17 (s, 2 H), 2.50 (s, 6H). FAB-MS ($[M+1]^+$): *m/z* 341. FAB-MS: 341.0 ([*M*+1]). Calc.: C, 67.45; H, 4.17; N, 15.49. Found: 67.03, 3.94, 15.63%.

2.5. Preparation of [Ru(2,9-dmp)$_2$(mip)](ClO$_4$)$_2$ · 2H$_2$O (**1**)

A mixture of *cis*-[Ru(2,9-dmp)$_2$(Cl)$_2$] · 2H$_2$O (294 mg, 0.5 mM), mip (170 mg, 0.5 mM) and ethylene glycol (30 ml) was thoroughly deoxygenated. The purple mixture was heated for 8 h at 120 °C under argon. When the solution finally turned brown, it was cooled to r.t., and an equal volume of sat. aq. $NaClO_4$ solution was added under vigorous stirring. The brownish solid was collected and washed with small amounts of H_2O, EtOH, and Et_2O, and dried at 50°. Purification by CC (Al_2O_3; MeCN/toluene 2:1).

Yield: 0.46 g (85%). UV (MeCN): 466 (12646), 271 (71091). ^{1}H NMR (400 MHz, (D_6)DMSO): δ = 8.91 (d, *J* = 8, 2H), 8.80 (d, *J* = 8, 2H), 8.44 (d, *J* = 8, 2H), 8.42 (d, *J* = 9, 2H), 8.24 (d, *J* = 9, 2H), 7.97 (d, *J* = 8, 2H), 7.79 (m, 2H), 7.49 (dd, 2H, J_1 = 5.5, J_2 = 5.5), 7.35 (t, 2H), 7.15 (d, *J* = 8.5, 1H), 7.33 (s,1H), 7.37 (d, *J* = 8, 2H). ESI-MS (MeCN): 957.1 ($[M-ClO_4]^+$), 857.3 ($[M-2ClO_4-H]^+$), 429.4 ($[M-2ClO_4]^{2+}$). Calc.: C, 52.54; H, 3.34; N, 10.03. Found: 52.76, 3.66, 10.25%.

2.6. Preparation of [Ru(4,7-dmp)$_2$(mip)](ClO$_4$)$_2$ (**2**)

Prepared in analogy to **1**, but from *cis*-[Ru(4,7-dmp)$_2$Cl$_2$] · 2H$_2$O (294 mg, 0.5 mM).

Yield 0.48 g (87%). UV (MeCN): 437 (24177), 262 (162221). ^{1}H NMR (500 MHz, ppm, (D_6)DMSO): δ 9.00 (d, *J* = 7, 2H), 8.46 (s, 4H), 7.92–7.97 (m, 6H), 7.89 (d, *J* = 1.5, 2H), 7.82 (d, *J* = 1.5, 1H), 7.75 (dd, 2H, J_1 = 5, J_2 = 5.5), 7.58 (t, 4H), 7.17 (d, *J* = 8.5, 1H), 6.15 (s, 2H), ESI-MS (MeCN): 957.1 ($[M-ClO_4]^+$), 857.4 ($[M-2ClO_4-H]^+$), 429.4 ($[M-2ClO_4]^{2+}$). Calc.: C, 52.51; H, 3.35; N, 10.01. Found: 52.76, 3.66, 10.25%.

3. Results and discussion

3.1. Synthesis and characterization

The ligand mip was synthesized on the basis of the method for imidazole ring preparation established by Steck and Day [32]. The complexes **1** and **2** were then prepared in yields of 85% and 87%, respectively, by direct reaction of mip with *cis*-[Ru(2,9-dmp)$_2$Cl$_2$]·2H$_2$O or *cis*-[Ru(4,7-dmp)$_2$Cl$_2$] · *n*H$_2$O, respectively, in the appropriate molar ratios, using ethylene glycol as solvent.

The desired Ru(II) complexes were isolated as the corresponding perchlorates, and were purified by column chromatography. In the ESI mass spectrum of **1**, the signals of $[M-ClO_4]^+$, $[M-2ClO_4-H]^+$, and $[M-2ClO_4]^{2+}$ were detected, and in the case of **2**, the signals for $[M-2ClO_4-H]^+$ and $[M-2ClO_4]^{2+}$ were observed. Both **1** and **2** gave rise to well-defined ^{1}H NMR spectra, permitting unambiguous identification and assessment of purity. The ^{1}H NMR chemical shifts were assigned by the aid of a ^{1}H, ^{1}H-COSY experiments, and by comparison with the values of similar compounds [19,33]. The chemical shifts of all the protons were presented in Experimental section. A full assignment was tentatively made for the multiplets in the region from 7.75 to 7.82 ppm. The proton resonance on the nitrogen atom of the imidazole ring was not observed, and it has been proposed that the proton exchanges quickly between the two nitrogens of the imidazole ring and it is a characteristic of an active proton [33a].

The UV–Vis absorption spectra of **1** and **2** in acetonitrile mainly consist of three resolved bands. The lowest energy absorption band at 466 nm (for complex **1**) or 437 nm (for complex **2**) assigned to metal-to-ligand charge transfer (MLCT) transition, and the other band at 271 nm (for complex **1**) or 262 nm (for complex **2**) is attributed to an intraligand (IL) $\pi \rightarrow \pi^*$ transition by comparison with the spectra of other polypyridyl Ru(II) complexes [33a, 34,35]. The highest energy absorption at 226 nm (for complex **1**) or 218 nm (for complex **2**) is unassigned at present, for it may be attributed to the MLCT [36,37] or $\pi \rightarrow \pi^*$ transition [38,39]. This indicates that the incorporation of electron-donating substituents at positions 2 and 9 in ring of the ancillary phen ligand shifts the MLCT band to longer wavelength, however, the result is on the contrary if the incorporation of electron-donating substituents at positions 4 and 7 in ring of the ancillary phen ligand. This phenomenon has also been found with other analogues [40].

Some trends in UV–Vis absorption spectra can be explained by the theoretical results. From Figs. 1 and 2, we can see that MO characterized by metal-orbital in the occupied frontier MO is NHOMO−2 (NHHOMO−2 = the next (next HOMO)) instead of HOMO, so that the λ_{max} of the ^{1}MLCT spectra band should be assigned to the electron transition from the NHOMO−2 to the LUMO. Such an assignment can be confirmed by the fact that the wavelength corresponding to the theoretical maximum of the ^{1}MLCT spectra band agrees with the experimental value. According to the approximate correlation if the reverse ratio of the energy difference ($\Delta\varepsilon_{L-H}$) between the LUMO and the HOMO−2 to the experimental wavelength (λ_{max}), using he parent complex $[Ru(bpy)_3]^{2+}$ as the standard (λ_{max} = 452 nm, $\Delta\varepsilon_{L-H}$ = 0.1239 atomic unit) [41] and $\Delta\varepsilon_{L-H}$ data of the two Ru(II) complexes **1** and **2** from Table 1, the computed λ_{max} values of the ^{1}MLCT absorption of **1** and **2** are 452 and 444 nm, respectively, near their λ_{exper} values of 466 nm and 437 nm, respectively.

The electrochemical behavior of complexes **1** and **2** were studied in MeCN by cyclic voltammetry (CV). Both complexes exhibit one oxidation and two reduction waves in the sweep range from −1.8 to +1.8 V, the half-wave potentials $E_{1/2}$, taken as the average of the cathodic peak E_{pc} being +1.34, −1.47, −1.63 V (versus SSCE) for complex **1** and +1.28, −1.35, −1.55 V for complex **2**. The electrochemical behavior of the Ru(Π) polypyridyl complex has been rationalized in terms of a metal-based oxidation and a series of reductions which are ligand-based occurring in a stepwise manner for each π^* system [42]. As expected, the incorporation of electron-donating methyl groups on the ancillary phen ligand shifts the Ru(II)/Ru(III) oxidation to the positive. These data are consistent with the electron donors stabilizing the Ru(II) state via raising the absolute energy of the highest occupied molecular orbital (HOMO) [38,43]. The above-mentioned electrochemical trends can be also explained by our theoretical results. The frontier molecular orbital energies and total energies, the schematic diagram of the energies and related ^{1}MLCT transition, and the molecular orbital stereographs of complexes **1** and **2** are given in Table 1, Figs. 2 and 3, respectively, based on the computed results. We can see that MO characterized by metal-orbital in the occupied frontier MO is NHOMO−2 instead of HOMO. Since the NHOMO−2 energy of

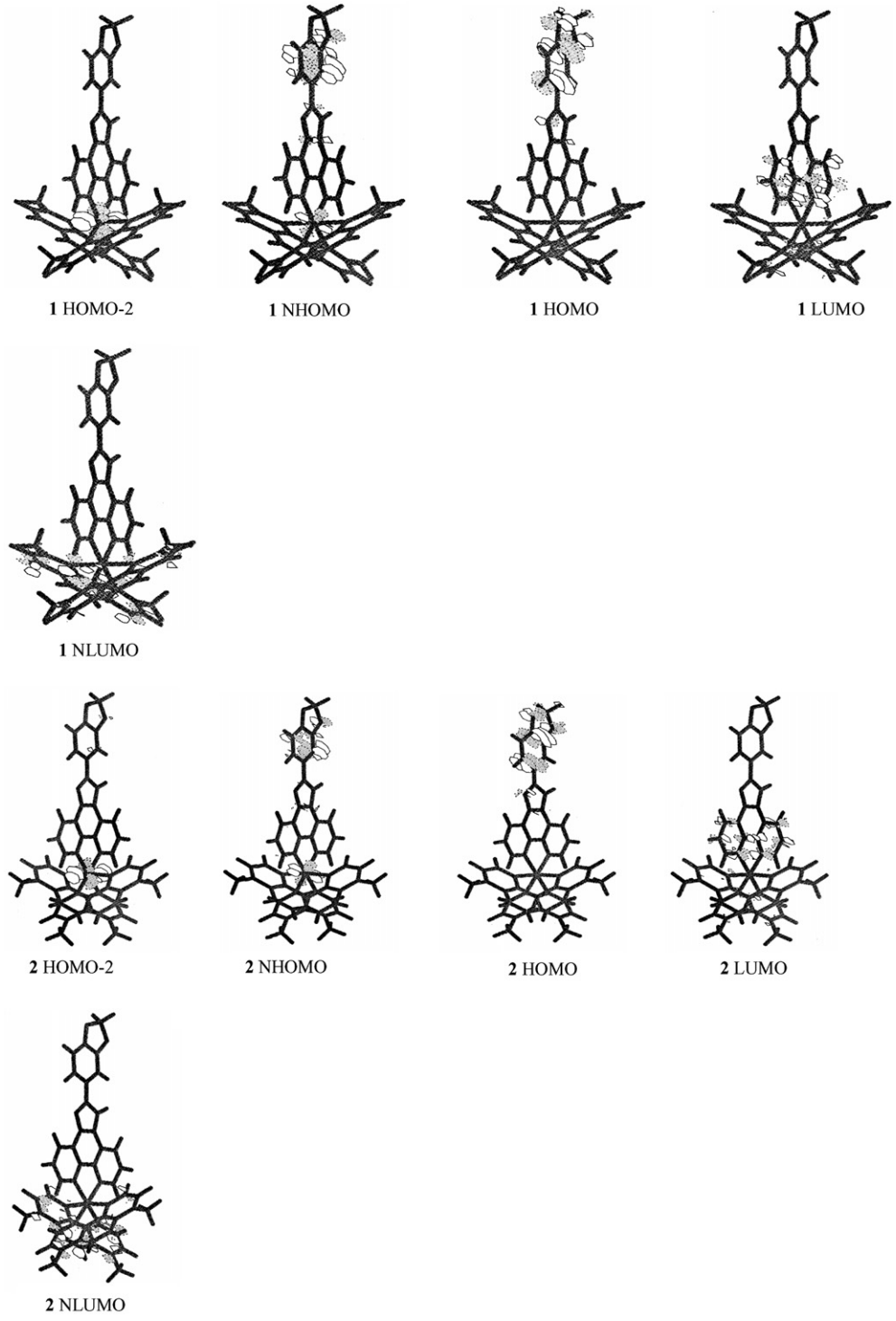

Fig. 1. Some related frontier molecular orbital stereographs of complex **1** and **2**.

complex **1** is lower than that of complex **2** (see Table 1 and Fig. 3), its oxidation potential is more positive than that of later.

3.2. UV–Vis titration

The interaction of complexes **1** and **2** with DNA was investigated by UV/VIS absorption. Fig. 3 shows the electronic spectral traces of the two complexes titrated with DNA (at constant concentration of complex). As the DNA concentration increases, for complex **1**, the pronounced hypochromism in the intraligand (IL) band reaches as high as 10.9% at 271 nm with a red shift of 2 nm at a [DNA]/[Ru] ratio of 6. The MLCT band at 469 nm shows hypochromism by about 13.1% and a red shift of 7 nm under the same experimental conditions. For complex **2**, upon addition of DNA, the IL band at 286 nm exhibits hypochromism of about 12.8% with a 2 nm red shift at a [DNA]/[Ru] ratio of 7 nm, the MLCT band at

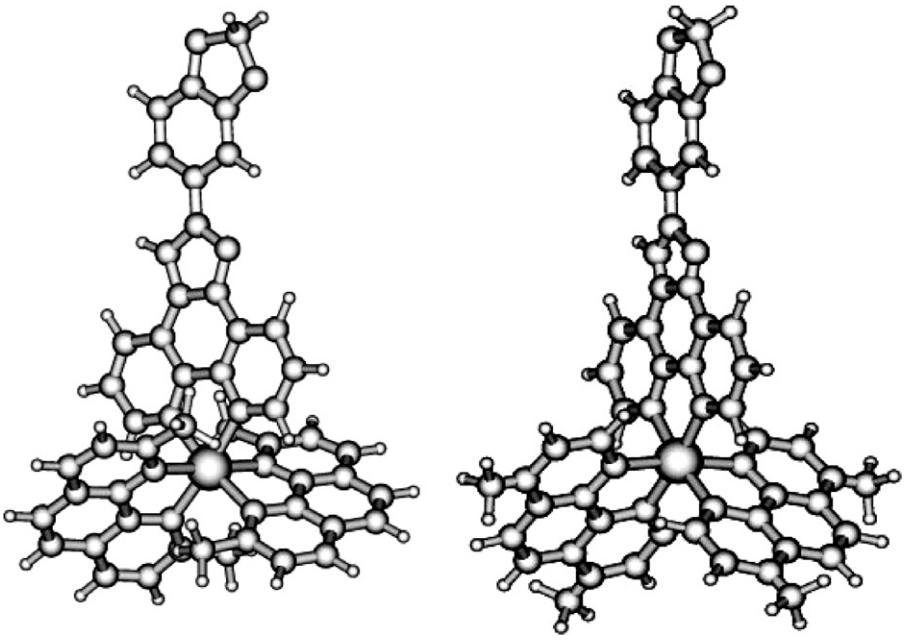

Fig. 2. The DFT-optimized structures and visualization of the orbitals of complex **1** (left) and **2** (right).

Table 1
Some frontier molecular orbital energies (ε_i/atomic unit) of complex **1** and **2** (1 atomic unit = 27.21 eV)

Compound	H-2	NHOMO	HOMO[a]	LUMO	Vir[b]	$\Delta\varepsilon_{L-H}$ [c]	$\Delta\varepsilon_{L-NH}$	$\Delta\varepsilon_{L-(H-2)}$	E_{Total}[d]
1	−0.3854	−0.3843	−0.3443	−0.2615	−0.2604	0.0828	0.1228	0.1228	−2532.5297
2	−0.3800	−0.3792	−0.3401	−0.2541	−0.2507	0.0860	0.1431	0.1230	−2532.5668

[a] Occ = occupied molecular orbital; HOMO (or H) = the highest Occ. NHOMO (or NH) = the next HOMO (or H-1).
[b] Vir = virtual molecular orbital; LUMO (or L) = the lowest Vir.
[c] $\Delta\varepsilon_{L-H}$ = energy difference between LUMO and HOMO, etc.
[d] E_{Total} = the total energy of complex.

441 nm shows hypochromism by about 16.2% and a red shift of 6 nm under the same experimental conditions. Comprising the hypochromism of the two complexes with that of their parent complex $[Ru(phen)_3]^{3+}$ (hypochromism in MLCT band at 445 nm of 12% and red shift of 2 nm [44], which interacts with DNA through a semi-intercalation or quasiintercalation [45]) and considering that the absorption spectrum of $[Ru(bpy)_3]^{2+}$, a typical electrostatic binding complex, was demonstrated to be unchanged upon the addition of the DNA [46], these spectral characteristics obviously suggest that both **1** and **2** in our paper interact with DNA most likely through a mode that involves a stacking interaction between the methylenediox chromophore and the base pairs of DNA. The spectra also imply that complex **2** binds to DNA more strongly than complex **1**.

To quantitatively compare the DNA-binging strengths of the two complexes, their intrinsic binding constants K_b were determined by UV–Vis titration. This was done by monitoring the change in absorbance at 469 nm for complex **1**, and at 445 nm for **2**, with increasing concentration of DNA, and by using [47]

$$[DNA]/(\varepsilon_a - \varepsilon_f) = [DNA]/(\varepsilon_b - \varepsilon_f) + 1/(K_b(\varepsilon_b - \varepsilon_f))$$

wherein [DNA] is the concentration of DNA in base pairs, ε_a, ε_f, and ε_b are the apparent-, free- and bound-metal-complex extinction coefficients, respectively. K_b is the equilibrium binding constant (in M^{-1}) of complex binding to DNA. When plotting $[DNA]/(\varepsilon_a - \varepsilon_f)$ versus [DNA], K_b is obtained by the ratio of the slope to the intercept. Thus, the intrinsic binding constants K_b of **1** and **2** were determined as $(2.1 \pm 0.12) \times 10^4$ and $(4.1 \pm 0.15) \times 10^4\ M^{-1}$, respectively. This results indicates that, as the ancillary ligand varies from 2,9-dmp to 4,7-dmp, the DNA-binding affinity of the Ru(II) complexes declines. For comparison, the intrinsic binding constants of typical 'intercalative-type' Ru(II) complexes is in the range of 1.18×10^4–$8.3 \times 10^4\ m^{-1}$ [48–50], whereas that of the parent complex $[Ru(phen)_3]^{2+}$ is $5.5 \times 10^3\ m^{-1}$ [4]. From the results, we could deduce that both **1** and **2** bind to DNA by intercalation. The intrinsic binding constants of **1** and **2** are bigger than that of $[Ru(phen)_3]^{2+}$, which can also be interpreted by the planarity area of the intercalated ligand. The planarity area (S) is $S_{mip} > S_{phen}$. In general, the extend π system of the intercalative ligand will increase the strength of interaction of the complexes with DNA [51].

3.3. Fluorescence quenching and competitive binding

Luminenescene spectroscopy is one of the most-common and most-sensitive ways to analyze drug–DNA interactions. Complex **1** showed no fluorescence emission, neither alone nor in the presence of CT-DNA. This could be caused by vibronic coupling between the methyls of 2,9-dmp ligand and solvent, leading to dissipation of energy in a non-radiative process. Similar results have observed for this type of Ru(II) complexes [50,52].

Steady-state completive binding experiment using complex **1** as quencher may give further information about the binding of the complex to DNA. Ethiduim bromide (EB) emits intense fluorescence light in the presence of DNA, due to its strong intercalation between adjacent DNA base pairs. It was previously reported that the enhanced fluorescence can be quenched, at least partially, by

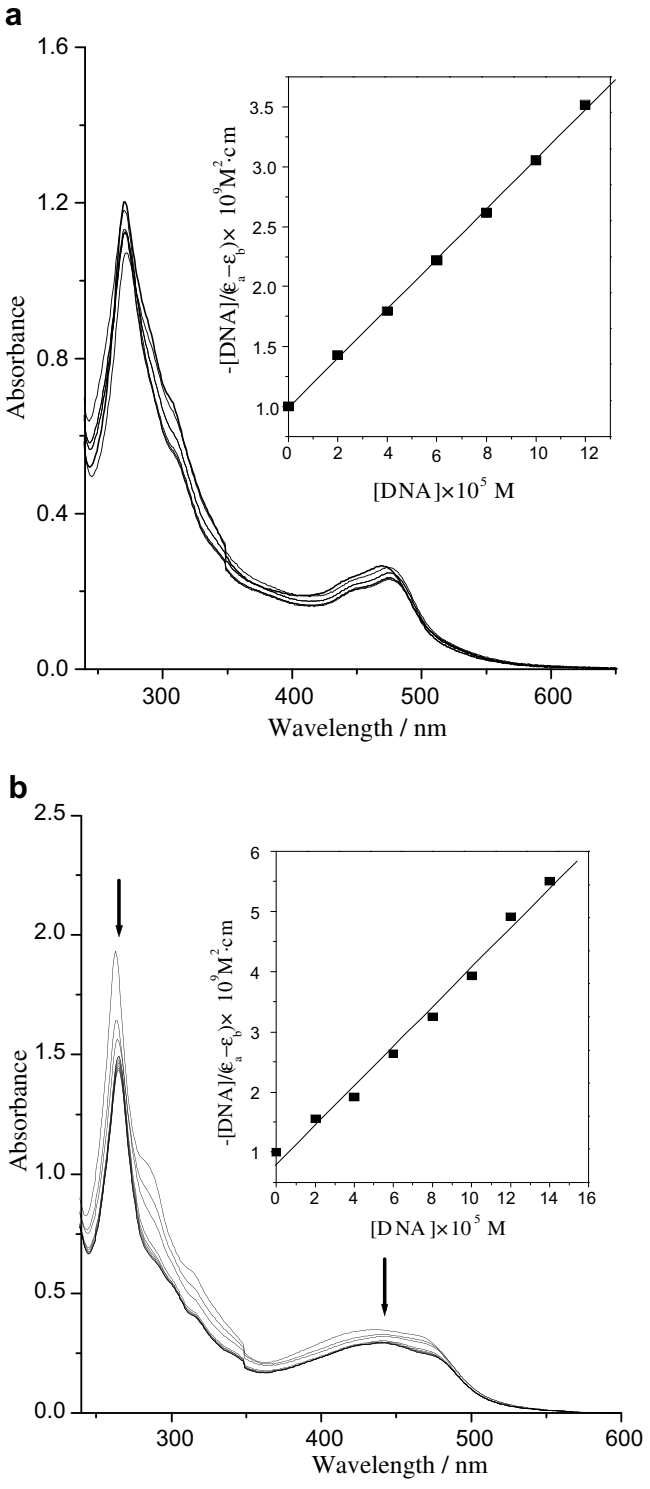

Fig. 3. Absorption spectra of the complexes **1** (a) and **2** (b) in Tris–HCl buffer upon addition of calf-thymus DNA. [Ru] = 2×10^{-5} M, [DNA] = $(0–86.68) \times 10^{-6}$ M. Arrow shows the absorbance changing upon increasing DNA concentrations. Plots of [DNA]/($\varepsilon_a - \varepsilon_f$) vs. [DNA] for the titration of DNA with the complex.

the addition of a second molecule [53]. The quenching extent of fluorescence of EB bound to DNA is used to determine the extent of binding of the second molecule to DNA. The emission spectra of EB bound to DNA in the absence and presence of **1** to DNA, pretreated with EB, causes appreciable reduction in emission intensity of 31.7% than that observed in the absence of **1** at a [Ru]/[DNA] ratio of 0.2.

The quenching plot illustrates that the removal of EB bound to DNA by complex **1** is in good agreement with the linear Stern–Volmer equation. The Stern–Volmer constant K (K is a liner Stern–Volmer quenching constant dependent on the ratio of the bound concentration of ethidium bromide to the concentration of DNA) was, thus, determined as 2.12, which is consistent with the UV–Vis-titration results (see above).

However, complex **2** can emit luminescence in the Tris buffer at ambient temperature, with a maximum at 603 nm, expecting that the hydrophobic methyl groups on the ancillary ligand would shield the 4,7-dmp nitrogens from the environment and thereby effectively preventing the solvent-quenching [54]. Upon addition of DNA, the emission intensity grows steadily and reaches 4.2 times larger than that of in the absence of DNA. For complex **2**, steady-state emission quenching experiments using $[Fe(CN)_6]^{4-}$ as quencher may give further information about its DNA-binding. The results indicate that in the absence of DNA, complex **2** was almost quenched by $[Fe(CN)_6]^{4-}$ completely. However, on addition of DNA, the Stern–Volmer plots changed drastically. The efficiency of $[Fe(CN)_6]^{4-}$ quenching of Ru(II) complex bound to DNA is decreased (relative to that of the free Ru(II) complex), which may be because the bound $[Ru(4,7\text{-dmp})_2(mip)]^{2+}$ cations is well protected from the anionic water-bound quencher by the array of negative charges along the DNA phosphate backbone (15a).

3.4. Viscosity studies

Further clarification of the interactions between the complexes and DNA was carried out by viscosity measurements. Photo-physical probes provide necessary, but not sufficient, clues to support a binding model. Hydrodynamic measurements that are sensitive to length change (i.e. viscosity and sedimentation) are regarded as the least-ambiguous and most-critical tests of binding model in solution, in the absence of crystallographic structural data (15). A classical intercalation model results in lengthening in the DNA helix, as base pairs are separated to accommodate the binding ligand, leading to the increase of DNA viscosity. However, a partial and/or non-classical intercalation of complex, such as $[Ru(phen)_3]^{2+}$, may bend (or link) DNA helix, reduce its effective length and, concomitantly, its viscosity [15,45]. In addition, some complexes such as $[Ru(bpy)_3]^{2+}$, which interacts with DNA by an electrostatic binding mode, have no influence on DNA viscosity [49]. The effects of complexes **1** and **2** on the viscosity of CT-DNA are showed in Fig. 4. As increasing the amounts of complex **1** or **2** are increased, the relative viscosity of DNA increases steadily, similar as in the case of EB. This increase in relative viscosity, expected to correlate with the compounds DNA-intercalating propensities, followed the order **2** > **1**. These results suggest that complexes **1** and **2** both bind to DNA through intercalation, the difference in binding strength probably being caused by the different ancillary ligands. The Me groups of the two dmp ligands in **1** are expected to give rise to much more steric hindrance than those in **2**. Therefore, complex **2** is probably more deeply intercalated and more tightly bound to adjacent DNA base pairs than complex **1**.

3.5. Enantioselective binding

Equilibrium-dialysis experiments offer the opportunity to examine the enantioselectivity of complexes binding to DNA. According to the proposed binding model by Barton and co-workers [55], the Δ enantiomer of the complex, a right-handed propeller-like structure, displays a greater affinity than the Λ enantiomer with the right-handed CT-DNA helix due to more- appropriate steric matching. We, thus, decided to test if the racemic complexes could be (partly) resolved in the presence of chiral CT-DNA. To this end, racemic solutions of the two complexes were dialyzed against

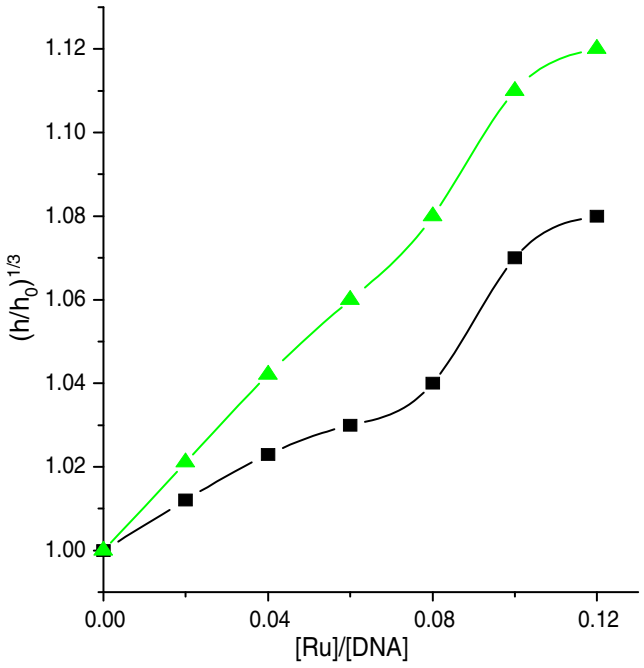

Fig. 4. Effect of the addition of increasing amounts of complex **1** (■) and **2** (▲) on the specific viscosity of calf-thymus DNA. The total DNA concentration: 0.5 mM, $T = 25\ (\pm 0.1)\ ^{\circ}C$.

CT-DNA for 60 h, and then subjected to circular-dichroism (CD) analysis. In Fig. 5, the CD spectra in the UV region of the dilysates of **1** or **2** are shown. The dilysates of **1** (solid line) shows two CD signals with a positive peak at 273 nm and a negative peak at 263 nm, while complex **2** (dotted line) shows weak CD signals with a positive peak at 267 nm and a negative peak at 258 nm, respectively.

Although neither of the complexes was resolved into the pure enantiomers, and we can not determine which enantiomer binds preferentially to CT-DNA, it is evident that both **1** and **2** interact enantioselectively with CT-DNA. The stronger CD signals of complex **1** suggest a large DNA-binding discrimination between its two antipodes. Since the intercalative ligands of **1** and **2** are the same, the difference should, again, be attributable to the ancillary ligands, more precisely, to the different substitution patterns of the 2,9-dmp moieties. These results, thus, clearly indicate that the substitution pattern of ancillary ligands can have a significant effect on the DNA-binding discrimination.

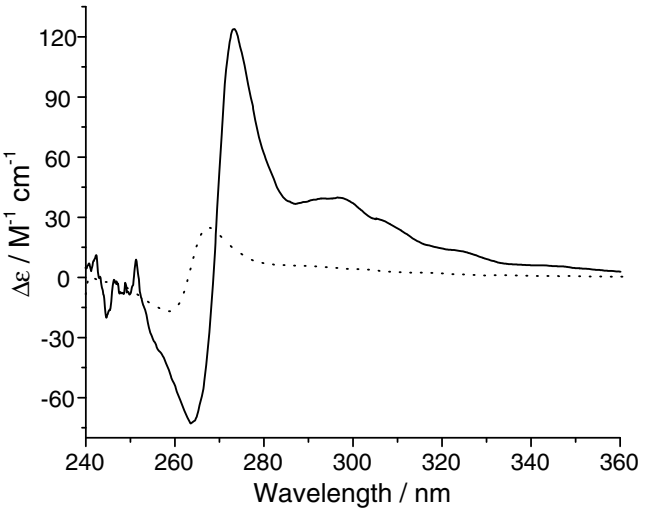

Fig. 5. CD spectra of **1** (—) and **2** (. . .) after 60 h dialysis against CT-DNA in stirred aq. solution. ([Ru] = 50 μM, [DNA] = 1.0 mM).

3.6. Theoretical explanation on the difference of DNA-binding of complexes *1* and *2*

The above-mentioned experimental results all showed that both complexes **1** and **2** can bind to DNA in intercalation mode and the DNA-binding affinity of complex **2** is greater than that of complex **1**. Since the intercalative ligands of both complexes are the same, the difference of DNA-binding affinity should be attributed to the ancillary ligand effects. It is very interesting that the ancillary ligands of the complexes are isomers and only the substitution sites of Me groups of 2,9-dmp and 4,7-dmp in **1** and **2** are different. The DFT calculations show that complex **2** is more stable than complex **1** in thermodynamics since the computed total energy of complex **2** is lower than that of complex **1** (see Table 1). However, the LUMO and NLUMO energies of complex **2** are greater than those of complex **1** to some extent (see Figs. 1 and 2). It has been documented that the lower LUMO energy of a complex in an intercalation mode is advantageous to the interaction between an intercalative ligand and DNA [53], and thus the greater LUMO energy of complex **2** is surely not advantageous to its DNA-binding affinity. However there are also two important factors affecting their DNA-binding properties. One is a hydrophobicity effect of an ancillary ligand and the other is a steric hindrance effect of an ancillary ligand. Obviously, the hydrophobicity of ancillary ligand 4,7-dmp in complex **2** is greater than that in **1**, and at the same time, its steric hindrance is smaller than that in **1**. These two factors are all advantageous to the DNA-binding of **2**, in particular, in the circumstances that an intercalative ligand containing a steric hindrance group (methylenedioxy) results in lower DNA-binding affinity relative to the parent ligand. It equals to that there is a greater exterior impetus for **2** than **1**, leading the intercalative ligand in **2** inserting more deeply between base pairs of DNA. Therefore, synthetically considering these factors, the difference of DNA-binding affinity of complex **1** and **2** [$K_b(\mathbf{2}) > K_b(\mathbf{1})$] can be well understood.

3.7. Photoactivated cleavage of pPR-322 DNA by complex *1* and *2*

There has been a great deal of interest in DNA endonucleolytic cleavage reactions that are activated by metal ions [56]. The delivery of high concentrations of metal ion to the helix, locally generating oxygen or hydroxide radicals, yields an efficient DNA cleavage reaction. The cleavage reaction on plasmid DNA can be monitored by agarose gel electrophoresis. When circular plasmid DNA is subject to electrophoresis, relatively, fast migration will be observed for the intact supercoil form (Form I). If scission occurs on one strand (nicking), the supercoil will relax to generate a slower-moving open circular form (Form Π). If both strands are cleaved, a linear form (Form III) that migrates between Form I and Form Π will be generated [57].

Fig. 6 shows gel electrophoresis separations of pBR-322 DNA after incubation with complex **1** and **2**, respectively, and irradiation at 365 nm. Lane 0 is the control group with DNA alone, no DNA gel-strand cleavage of supercoiled Form I to nicked Form Π happens. With increasing concentration of complex **1** (a) or **2** (b) (lanes 1–4), Form I of pBR-322 DNA diminishes gradually, whereas the amount of Form Π increases. Complex 1 induces the single-strand scissions in supercoiled DNA, however, at the concentration of 40 μM, complex **2** can almost promote the complete conversion of DNA from Form I to Form Π (6, b, lane 4). Fig. 7 shows the gel electrophoretic separations of pBR-322 DNA after incubation with

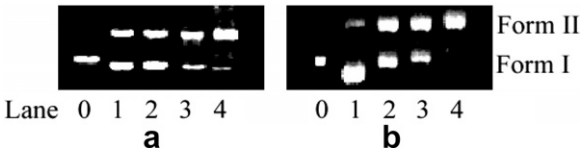

Fig. 6. Photoactivated cleavage of pBR-322 DNA in the absence and presence of the complex **1** (a) or **2** (b) after 60 min irradiation at 365 nm. Lane 0, in DNA alone; lanes (1–4), at 5, 10, 20, and 40 μM Ru(II) complexes, respectively.

Fig. 7. Photocleavage of pBR-322 DNA in the presence of the complex **1** (20 μM, a) or **2** (20 μM, b) after different times irradiation at 365 nm. Lanes (1–4), at 20, 40, 60, and 80 min, respectively.

complex **1** and **2**, respectively, and irradiation at 365 nm for variable times. It takes 80 min irradiation for complex **1** to promote the complete conversion of plasmid DNA from Form I to Form Π (Fig. 7, a, lane 4), however, a shorter irradiation time, just 60 min for complex **2** to promote the complete cleavage of plasmid DNA (Fig. 7, b, lane 3). The results indicate that **2** is more effective in clearing DNA than **1**. This may be related to the molecular of these complexes, which has been testified in other cases [58]. However, it is necessary to further study on clarifying the reaction mechanism.

4. Conclusions

Two novel Ru(II) complexes of $[Ru(2,9\text{-dmp})_2(mip)]^{2+}$ (**1**) and $Ru(4,7\text{-dmp})_2(mip)]^{2+}$ (**2**) have been synthesized and characterized. The experimental results indicate that both complexes bind to DNA in an intercalation mode, and they are efficient photosensitisers for cracking DNA plasmid. Furthermore, ancillary ligands have an important effect on the DNA-binding and photocleavage properties of the complexes, and lead the order of DNA-binding affinity (A) of the complexes being $A(\mathbf{2}) > A(\mathbf{1})$.

Acknowledgements

We thank the Provincial Natural Science Fund of Hunan (06JJ50023), the Scientific Research Found of Hunan Provincial Education Department (08B086), and the Doctoral Foundation of Xiangtan University (05QDZ11) for financial support.

References

[1] A. Sigel, H. Sigel (Eds.), Metal Ions in Biological Systems, vol. 33, Marcel Dekker, New York, 1996.
[2] K.E. Erkkila, D.T. Odom, J.K. Barton, Chem. Rev. 99 (1999) 2777.
[3] L.N. Ji, Q.L. Zhang, H. Chao, Chinese Sci. Bull. 46 (2001) 1332.
[4] A.M. Pyle, J.P. Rehmann, R. Meshoyrer, C.V. Kumar, N.J. Turro, J.K. Barton, J. Am. Chem. Soc. 111 (1989) 3051.
[5] (a) E. Tuite, P. Lincolin, B. Nordén, J. Am. Chem. Soc. 119 (1997) 239;
(b) L.M. Wilhelmsson, F. Westerlund, P. Lincoln, B. Nordén, J. Am. Chem. Soc. 124 (2002) 12092.
[6] X.J. Yang, F. Drepper, B. Wu, W.H. Sun, W. Haehnel, C. Janiak, J. Chem. Soc., Dalton Trans. (2005) 256.
[7] L.F. Tan, F. Wang, H. Chao, Helv. Chim. Acta 90 (2007) 205.
[8] X.W. Liu, J. Li, H. Li, K.C. Zheng, H. Chao, L.N. Ji, J. Inorg. Biochem. 99 (2005) 2372.
[9] (a) P.U. Maheswari, V. Rajendiran, M. Palaniandavar, R. Parthasarathi, V. Subramanian, J. Inorg. Biochem. 100 (2006) 3;
(b) P. Nagababu, J.N.L. Latha, S. Satyanarayana, Chem. Biodivers., 3 1219 (2006);
(c) S. Shi, J. Liu, J. Li, K.C. Zheng, X.M. Huang, C.P. Tan, L.M. Chen, L.N. Ji, J. Inorg. Biochem. 100 (2006) 385.
[10] (a) J. Liu, W. J Zheng, S. Shi, C.P. Tan, J.C. Chen, K.C. Zheng, L.N. Ji, J. Inorg. Biochem. 102 (2008) 193;
(b) L.M. Chen, J. Liu, J.C. Chen, C.P. Tan, S. Shi, K.C. Zheng, L.N. Ji, J. Inorg. Biochem. 102 (2008) 330.
[11] Y. Jenkins, A.E. Friedman, N.J. Turro, J.K. Barton, Biochemistry 31 (1992) 10809.
[12] E.J.C. Oison, D. Hu, A. Hormann, A. Jonkman, M.R. Arkin, E.D.A. Stemp, J.K. Barton, P.F.J. Barbara, J. Am. Chem. Soc. 119 (1997) 11458.
[13] (a) H. Dong, H. Xu, Y. Yang, H. Li, H. Zou, L.H. Qu, L.N. Ji, J. Inorg. Biochem. 97 (2003) 207;
(b) H. Dong, J.W. Cai, H. Zhang, L.N. Ji, J. Chem. Soc., Dalton Trans. (2003) 325.
[14] (a) M. Eriksson, M. Leijon, C. Hiort, B. Norden, A. Graslund, Biochemistry 33 (1994) 5031;
(b) M. Eriksson, M. Leijon, C. Hiort, B. Norden, A. Graslund, J. Am. Chem. Soc. 114 (1992) 4933;
(c) C. Hiort, B. Norden, A. Rodger, J. Am. Chem. Soc. 112 (1990) 1971.
[15] (a) S. Satyanarayana, J.C. Dabrowiak, J.B. Chaires, Biochemistry 31 (1992) 9319;
(b) S. Satyanarayana, J.C. Dabrowiak, J.B. Chaires, Biochemistry 32 (1993) 2573.
[16] J.E. Coury, J.R. Anderson, L. McFail-Isom, L.D. Williams, L.A. Bottomley, J. Am. Chem. Soc. 119 (1997) 3792.
[17] (a) Y. Xiong, X.F. He, X.H. Zou, J.Z. Wu, X.M. Chen, L.N. Ji, R.H. Li, J.Y. Zou, K.B. Yu, J. Chem. Soc., Dalton Trans. (1999) 19;
(b) J.Z. Wu, G. Yang, S. Chen, L.N. Ji, J.Y. Zhou, Y. Xu, Inorg. Chim. Acta 283 (1998) 17.
[18] D. Lawrence, V.G. Vaidyanathan, B.U. Nair, J. Inorg. Biochem. 100 (2006) 1244.
[19] L.F. Tan, H. Chao, Inorg. Chim. Acta 360 (2007) 2016.
[20] B.P. Sullivan, D.J. Salmon, T.K.J. Meyer, Inorg. Chem. 17 (1978) 3334.
[21] J.N. Barddock, T.J. Meyer, J. Am. Chem. Soc. 95 (1973) 3158.
[22] M. Yamada, Y. Tanaka, Y. Yoshimato, S. Kuroda, I. Shimao, Bull. Chem. Soc. Jpn. 65 (1992) 1006.
[23] J. Marmur, J. Mol. Biol. 3 (1961) 208.
[24] M.F. Reichmann, S.A. Rice, C.A. Thomas, P. Doty, J. Am. Chem. Soc. 76 (1954) 3047.
[25] J.B. Chairs, N. Dattagupta, D.M. Crothers, Biochemistry 21 (1982) 3933.
[26] G. Cohen, H. Eisenberg, Biopolymers 8 (1969) 45.
[27] A.D. Becke, J. Chem. Phys. 98 (1993) 1372.
[28] A. Gorling, Phys. Rev. A 54 (1996) 3912.
[29] A. Juris, V. Balzani, F. Barigeletti, S. Campagna, P. Belser, A. von Zelewsky, Coord. Chem. Rev. 84 (1988) 85.
[30] M.J. Frisch, G.W. Trucks, H.B. Schlegel, G.E. Scuseria, M.A. Robb, J.R. Cheeseman, S. Dapprich, J.M. Millam, A.D. Danieks, K.N. Kudin, M.C. Strain, O. Farkaas, J. Tomasi, V. Barone, M. Cossi, R. Cammi, B. Mennucci, C. Pomelli, C. Adamo, S. Clifford, J. Ochterski, G.A. Petersson, P.Y. Ayala, D.K. Maallic, A.D. Rabuck, K. Raghavachari, J.B. Forresman, J. Cioslowski, J.V. Piskorz, I. Komaromi, R. Gomperts, R.L. Martin, D.J. Fox, T. Keith, M.A. Al-Laham, C.Y. Peng, A. Nanayakkara, M. Challacombe, P.M.W. Gill, B. Johanson, W. Chen, M.W. Wong, J.A. Pople, GAUSSIAN 98, Revision A.11.4, GAUSSIAN, Inc., Pittsburgh, PA, 2002.
[31] G. Schaftenaar, MOLDEN v3.6 program, CMBI, Faculty of Science, 2002.
[32] E.A. Steck, A.R. Day, J. Am. Chem. Soc. 65 (1943) 452.
[33] (a) J.Z. Wu, B.H. Ye, L. Wang, L.N. Ji, J.Y. Zhou, R.H. Li, Z.Y. Zhou, J. Chem. Soc., Dalton Trans. (1997) 1395;
(b) R.B. Nair, E.S. Teng, S.L. KirKland, C. Murphy, J. Inorg. Chem. 37 (1998) 139.
[34] J. Fees, W. Kaim, M. Moscherosch, W. Matheis, J. Klima, M. Krejcik, S. Zails, Inorg. Chem. 32 (1993) 166.
[35] K. Kalyanasundaram, Coord. Chem. Rev. 46 (1982) 159.
[36] J.C. Chambron, J.-P. Sauvage, Chem. Phys. Lett. 182 (1991) 603.
[37] E. Amouyal, A. Homsi, J.C. Chambron, J.-P. Sauvage, J. Chem. Soc., Dalton Trans. (1990) 1384.
[38] D.P. Rillema, G. Allen, T.J. Meyer, D.C. Conrad, Inorg. Chem. 22 (1983) 1617.
[39] D.P. Rillema, C.B. Balanton, R.J. Shaver, D.C. Jackman, M. Moldaji, S. Bundy, L.A. Worl, T.J. Meyer, Inorg. Chem. 31 (1992) 1600.
[40] R.E. Holmlin, J.A. Yao, J.K. Barton, Inorg. Chem. 38 (1999) 174.
[41] K.C. Zheng, J.P. Wang, W.L. Peng, X.W. Liu, F.C. Yun, J. Phys. Chem. A 105 (2001) 10899.
[42] B.K. Ghosh, A. Chakravorty, Coord. Chem. Rev. 95 (1989) 239.
[43] J.R. Schoonover, W.D. Bates, T.J. Meyer, Inorg. Chem. 34 (1995) 6421.
[44] L.N. Ji, X.H. Zou, J.G. Liu, Coord. Chem. Rev. 216–217 (1999) 513.
[45] P. Lincoln, B. Norden, J. Phys. Chem. B 102 (1998) 9583.
[46] G. Yang, J.Z. Wu, L. Wang, L.N. Ji, X. Tian, J. Inorg. Biochem. 66 (1997) 141.
[47] A. Wolf, G.H. Shimer Jr, T. Meehan, Biochemistry 26 (1987) 6392.
[48] X.H. Zou, B.H. Ye, L.Q. Zhang, H. Chao, J.G. Liu, L.N. Ji, X.Y. Li, J. Biol. Inorg. Chem. 6 (2001) 143.
[49] J.G. Liu, B.H. Ye, H. Li, Q.X. Zhen, L.N. Ji, Y.H. Fu, J. Inorg. Biochem. 76 (1999) 265.
[50] H. Xu, K.C. Zheng, Y. Cheng, Y.Z. Li, L.J. Lin, H. Li, P.X. Zhang, L.N. Ji, J. Chem. Soc., Dalton Trans. (2003) 2260.
[51] Y. Xiong, L.N. Ji, Coord. Chem. Rev. 185–186 (1999) 711.
[52] J.G. Liu, Q.L. Zhang, X.F. Shi, L.N. Ji, Inorg. Chem. 40 (2001) 50445.

[53] (a) J.R. Lakowicz, G. Webber, Biochemistry 12 (1973) 4161;
(b) B.C. Baguley, M. Lebret, Biochemistry 23 (1984) 937.
[54] Nobuko Komatsuzaki, Ryuzi Katoh, Yuichiro Himeda, Hideki Sugihara, Hironori Arakawa, Kazuyuki Kasuga, J. Chem. Soc., Dalton Trans. 20 (2000) 3053.
[55] (a) J.K. Barton, J.J. Dannenberg, A.L. Raphael, J. Am. Chem. Soc. 106 (1984) 2172;
(b) J.K. Barton, Science 233 (1986) 727.
[56] (a) R.P. Hertzberg, P.B. Dervan, J. Am. Chem. Soc. 104 (1982) 313;
(b) D.S. Sigman, D.R. Graham, L.E. Marshall, K.A. Reich, J. Am. Chem. Soc. 102 (1980) 5419.
[57] J.K. Barton, A.L. Raphael, J. Am. Chem. Soc. 106 (1984) 2466.
[58] (a) X.W. Liu, J. Li, H. Li, K.C. Zheng, H. Chao, L.N. Ji, J. Inorg. Biohem. 100 (2006) 385;
(b) H. Chao, W.J. Mei, Q.W. Huang, L.N. Ji, J. Inorg. Biohem. 92 (2002) 165.